

Statistics of Superluminal Motion in Active Galactic Nuclei *

Yong-Wei Zhang and Jun-Hui Fan

Center for Astrophysics, Guangzhou University, Guangzhou 510006, China; *fjh@gzhu.edu.com*

Received 2007 September 13; accepted 2007 December 18

Abstract We have collected an up-to-date sample of 123 superluminal sources (84 quasars, 27 BL Lac objects and 12 galaxies) and calculated the apparent velocities (β_{app}) for 224 components in the sources with the Λ -CDM model. We checked the relationships between their proper motions, redshifts, β_{app} and 5 GHz flux densities. Our analysis shows that the radio emission is strongly boosted by the Doppler effect. The superluminal motion and the relativistic beaming boosting effect are, to some extent, the same in active galactic nuclei.

Key words: galaxies: jets — galaxies: general — BL Lacertae objects: active — quasars: data analysis

1 INTRODUCTION

The observational properties of active galactic nuclei (AGNs) attract much interest. Their variability, high and variable polarization, variable high energetic gamma-ray emissions and superluminal motion strongly suggest the effect of relativistic beaming (see Blandford et al. 1977; Hartman et al. 1999; Xie et al. 2001; Fan et al. 1996; Fan et al. 1999; Fan et al. 2004; Fan et al. 2005). Superluminal motion is a piece of observational evidence for the beaming effect.

With the advent of very large baseline interferometry (VLBI) in radio astronomy in the late 1960s and early 1970s, it became possible to measure the structure of radio sources on angular scales of milliarcseconds. One of the early observational results of VLBI was that some compact radio sources were made up of more than one component, and that these components seem to be separating at apparent velocities greater than the speed of light. A number of possible explanations (see Blandford et al. 1977) have been proposed for such motion. Vermeulen & Cohen (1994) and Shen et al. (2001) stated that many active galactic nuclei contain compact radio sources with several components that appear to move apart in successive high-resolution VLBI images. When the apparent transverse velocity of separation exceeds the velocity of light ($\beta_{app} \equiv v/c > 1$), the motion and the object are said to be superluminal. They listed 66 such extragalactic sources and investigated several modifications to the simple relativistic beaming concept, they also checked separately the distribution of β_{app} in lobe-selected and core-selected quasars. Fan et al. (1996) compiled a sample of superluminal motion sources, and investigated the beaming effect. Kellermann et al. (2003) reported preliminary results of a seven-year long VLBA observational program and gave a sample of 96 superluminal sources in their study of the nature of the beaming effect in blazars; they found that in a few sources the motion appears to be directed inward, most likely the result of projection of a curved trajectory which bends back along the line of sight. The apparent motion of the jet features is not always oriented along the line joining the feature to the core. Very recently, Cohen, Lister & Vermeulen (2005) examined Doppler boosting and superluminal motion for 110 superluminal sources in the 15 GHz VLBA survey, and found that the distribution of the Doppler factor δ peaks at some low value and decreases to $\delta \sim 30$. The Lorentz factor Γ is a more fundamental quantity than δ , but it is harder to estimate. Also a comparison of

* Supported by the National Natural Science Foundation of China.

β_{app} and δ shows that the superluminal velocity and the variability Doppler factors are roughly consistent with the standard relativistic motion.

In spite of decades of study of superluminal sources, the details of the kinematics have remained elusive. One of the problems is that contrary to indications of early observations, the radio jets often do not contain simple, well-defined moving components (e.g., Cohen et al. 1977). Instead, the jets may show a complex brightness distribution with regions of enhanced intensity that may brighten and fade with time (Kellermann et al. 2003). Some features appear to move, others are stationary, or may break up into two or more separate features, and it is often unclear how these moving features are related to the actual underlying relativistic flow. Very recently, Shen et al. (2005) presented the results from the first quasi-simultaneous multi-frequency (2.3, 5.0, 8.4, and 15 GHz) VLBI observations of a compact steep-spectrum (CSS) superluminal source, 3C 138. For the first time, the spectral distribution of the components within its central 10 milliarcsecond (mas) region was obtained. The possibility that none of these visible components is the true core is also discussed. The present sample consists of 123 superluminal sources: a statistical analysis of these should be interesting.

Through out this paper, the Λ -CDM model (Pedro 2007) with $\Omega_\Lambda \simeq 0.7$, $\Omega_M \simeq 0.3$ and $\Omega_K \simeq 0.0$, and the relativistic beaming model are used, also we use the Hubble parameter $H_0 \simeq 75 \text{ km s}^{-1} \text{ Mpc}^{-1}$.

2 SAMPLE OF SUPERLUMINAL SOURCES AND SOME STATISTICAL RESULTS

2.1 The Sample

The original source of the present sample is based on Vermeulen & Cohen (1994) as supplemented by Kellermann et al. (2003) and Cohen, Lister & Vermeulen (2005). Our goal is to include all published superluminal sources, for which we have collected the proper motions and computed the apparent velocities (β_{app}) in the Λ -CDM model. The present sample consists of 224 components in 123 sources (84 quasars, 27 BL Lac objects and 12 galaxies). Many of the sources contain more than one component with measured proper motion. In order to relate our observations to the relativistic beaming model, we have to define a complete, un-biased, and flux density-limited sample. However, since AGNs are always variable, there is no simple objective way of obtaining a precisely defined flux density-limited sample (Kellermann et al. 2003). So we choose the latest data of the flux density at 5 GHz in following discussion. All the data are listed in Table 1. Here, column 1 gives the International Association of Universities (IAU) name; column 2 the classification (all sources have been classified as one of three types: Q the quasar, G the galaxy, and B the BL Lac object, C1, C2, … C8 stand for the individual components which some authors denote by A–E, K, J and S. In the present paper, we directly used the component identification from the literature. The quasar suffixes are: c for core-selected, l for lobe-selected and p for compact symmetric); columns 3 and 4 are the redshift and the corresponding references; columns 5 and 6 give the proper motion and references. For some sources the proper motions are not available in the literature: they were then calculated from the apparent velocities by the formulae in the original paper: they are: 0420–022 from Hong et al. (1999), 1038+528 from Marcaide et al. (1985), 1156+106 from Piner & Kingham (1997), 1606+106 from Piner & Kingham (1998), 1611+343 from An et al. (2001); column 7 is β_{app} , computed by

$$\beta_{\text{app}} = \frac{\mu}{H_0} \int_1^{1+z} \frac{1}{\sqrt{\Omega_M x^3 + 1 - \Omega_M}} dx. \quad (1)$$

We always used the fastest β_{app} value in our analysis. We did not include the following sources: 0833+654 and 0835+580 (with negative β_{app}) and 0839+616 and 1607+268 (zero β_{app}).

2.2 Statistical Results

2.2.1 The Relation between Proper Motion and Redshift

Superluminal motion is common in active galactic nuclei (Kembhavi & Narlikar 1999). Here, we investigate the relationship between the proper motion and redshift for the three types of objects (quasars, BL Lacs and galaxies). See Figure 1. When we consider the three types separately, we find: for the quasars, the redshifts range from 0 to 2.5, the proper motions, from 0 to 0.6. For the BL Lacs, the redshifts from 0 to 1 and the proper motions from 0 to 1.5. For the galaxies, the redshifts from 0 to 0.15 and the proper motion from 0 to 4. For the whole sample, we found $\log \mu = -(0.28 \pm 0.11) \log z - (0.75 \pm 0.28)$, with a linear correlation coefficient of –0.26.

Table 1 The 224 Individual Feature Data of 123 Superluminal Sources

IAU name	classification	z	references	μ	references	β_{app}	$S_{5 \text{ GHz}}^{\text{ob}} (\text{Jy})$	ref
0016+731	Q_c	1.781	VC94	0.22 ± 0.05	VC94	15.8 ± 3.79	1.7	HF04
0035+413	Q,B	1.353	Kell04	0.1 ± 0.02	Kell04	6.03 ± 1.21	1.1	HF04
0055+300	G,B	0.0165	Kell04	0.14 ± 0.02	Kell04	0.15 ± 0.02	0.59	VC94
0059+581	Q	0.643	Pya03	1.2	Pya98	41.5	3.26	Bec91
0106+013	Q_c	2.017	VC94	0.2 ± 0.05	VC94	15.4 ± 3.85	3.4	HF04
0108+388	G	0.67	VC94	0.1	VC94	3.57	1.3	HF04
0133+207	Q_l	0.425	VC94	0.24 ± 0.05	VC94	5.81 ± 1.21	0.07	VC94
0149+218	Q,C	1.32	Kell04	0.29 ± 0.04	Kell04	17.2 ± 2.37	1.1	HF04
0153+744	Q_c,C2	2.338	VC94	0.02 ± 0.04	VC94	1.66 ± 3.58	—	—
0153+744	Q_c,C3	2.338	VC94	0.08 ± 0.22	VC94	6.66 ± 18.3	1.5	HF04
0153+744	Q_c,C4	2.338	VC94	-0.12 ± 0.22	VC94	-9.99 ± 18.3	—	—
0202+149	Q_c	0.833	SRK96	0.18 ± 0.01	PMM00	7.65 ± 0.43	2.7	HF04
0208-512	Q	1.003	PJW76	0.6	SHW98	29.4	1.342	Fos98
0212+735	Q_c,C2	2.367	VC94	0.09 ± 0.05	VC94	7.54 ± 4.19	3.2	HF04
0212+735	Q_c,C3	2.367	VC94	0.07 ± 0.19	VC94	5.86 ± 15.9	—	—
0212+735	Q_c,C4	2.367	VC94	-0.14 ± 0.29	VC94	-11.7 ± 24.3	—	—
0219+428	B,C4	0.444	Mil78a	0.57 ± 0.14	JM01	14.3 ± 3.52	—	—
0219+428	B,C3	0.444	Mil78a	0.82 ± 0.03	JM01	20.6 ± 0.75	—	—
0219+428	B,C2	0.444	Mil78a	1.11 ± 0.2	JM01	27.9 ± 5.03	0.78	Fos98
0234+285	Q_c,B	1.207	Kell04	0.25 ± 0.05	Kell04	13.96 ± 2.79	3.4	HF04
0235+164	B,C1	0.94	PBE06	0.51 ± 0.14	PBE06	23.8 ± 6.53	1.9	HF04
0235+164	B,C2	0.94	PBE06	0.18 ± 0.03	PBE06	8.39 ± 1.4	—	—
0235+164	B,C3	0.94	PBE06	0.16 ± 0.09	PBE06	7.46 ± 4.19	—	—
0316+413	G	0.017	VC94	0.54 ± 0.12	VC94	0.58 ± 0.13	42.4	HF04
0333+321	Q_c,B	1.263	Kell04	0.18 ± 0.01	Kell04	10.4 ± 0.58	2	HF04
0333+321	Q_c,C	1.263	Kell04	0.2 ± 0.02	Kell04	11.5 ± 1.15	—	—
0336-019	Q_c	0.852	Kell04	0.22 ± 0.04	Kell04	9.52 ± 1.73	3	HF04
0415+379	G,D	0.0485	Kell04	1.52 ± 0.04	Kell04	4.61 ± 0.12	5.17	Gur99
0420-022	Q	0.915	Hong99	0.035	Hong99	1.6	1.22	Zen02
0420-014	Q	0.92	Von95	0.15	SWH97	6.88	4.4	HF04
0430+052	G,A	0.033	VC94	1.35	VC94	2.8	—	—
0430+052	G,B	0.033	VC94	2.53	VC94	5.25	—	—
0430+052	G,C	0.033	VC94	2.47	VC94	5.12	—	—
0430+052	G,D	0.033	VC94	2.66	VC94	5.51	3.8	HF04
0430+052	G,E	0.033	VC94	2.54	VC94	5.27	—	—
0440-003	B	0.844	JM01	0.34 ± 0.03	JM01	14.6 ± 1.29	1.32	Fos98
0454+844	B	0.112	Kell04	0.14 ± 0.04	VC94	0.97 ± 0.28	1.1	HF04
0458-020	Q_c	2.27	PK06	0.15 ± 0.01	JM01	12.3 ± 0.82	3.3	HF04
0528+134	Q_c,C1	2.07	BW99	0.15 ± 0.03	BW99	11.7 ± 2.34	6.2	HF04
0528+134	Q_c,C2	2.07	BW99	0.14 ± 0.03	BW99	10.9 ± 2.34	—	—
0528+134	Q_c,C3	2.07	BW99	0.12 ± 0.01	BW99	9.36 ± 0.78	—	—
0528+134	Q_c,C4	2.07	BW99	0.13 ± 0.01	BW99	10.1 ± 0.78	—	—
0528+134	Q_c,C5	2.07	BW99	0.13 ± 0.01	BW99	10.1 ± 0.78	—	—
0552+398	Q_p	2.365	VC94	0.04 ± 0.02	VC94	3.35 ± 1.67	4.9	VC94
0615+820	Q_c	0.71	VC94	0.05 ± 0.05	VC94	1.87 ± 1.87	1	HF04
0637-752	Q	0.651	Igu00	0.073	Igu00	2.55	3.05	Fos98
0710+439	G	0.518	VC94	0.003 ± 0.008	VC94	0.09 ± 0.23	1.6	HF04
0716+714	B,C2	0.3	BK05	1.1 ± 0.15	JM01	19.4 ± 2.65	—	—
0716+714	B,C3	0.3	BK05	1.2 ± 0.2	JM01	21.2 ± 3.53	0.93	Fos98
0716+714	B,C4	0.3	BK05	0.9	JM01	15.9	—	—
0723+679	Q_l	0.846	VC94	0.19	VC94	8.18	0.32	VC94
0735+178	B,C0	0.424	VC94	0.44 ± 0.03	VC94	10.6 ± 0.72	2.2	HF04
0736+017	Q,B	0.191	Kell04	0.96 ± 0.04	Kell04	11.1 ± 0.46	1.8	HF04
0736+017	Q,D	0.191	Kell04	0.39 ± 0.06	Kell04	4.51 ± 0.69	—	—
0736+017	Q,E	0.191	Kell04	0.86 ± 0.09	Kell04	9.94 ± 1.04	—	—
0738+313	Q,B	0.63	Kell04	0.07 ± 0.01	Kell04	2.38 ± 0.34	3.4	HF04
0745+241	Q,C	0.409	Kell04	0.33 ± 0.04	Kell04	7.72 ± 0.94	1.2	HF04
0748+126	Q,B	0.889	Kell04	0.12 ± 0.01	Kell04	5.36 ± 0.45	1.9	HF04
0754+100	B,B	0.266	Kell04	0.76 ± 0.13	Kell04	12 ± 2.05	0.9	Gur99
0814+425	B,B	0.245	Kell04	0.18 ± 0.02	Kell04	2.63 ± 0.29	1.9	HF04

Table 1 – Continued

IAU name	classification	z	references	μ	references	β_{app}	$S_{5 \text{ GHz}}^{\text{ob}} (\text{Jy})$	ref
0823+033	B,C	0.506	Kell04	0.48 ± 0.04	Kell04	13.5 ± 1.13	1.9	HF04
0823+033	B,D	0.506	Kell04	0.31 ± 0.05	Kell04	8.74 ± 1.41	–	–
0827+243	Q,C2	0.939	PBE06	0.51 ± 0.09	PBE06	23.8 ± 4.19	0.67	Fos98
0827+243	Q,C3	0.939	PBE06	0.38 ± 0.07	PBE06	17.7 ± 3.26	–	–
0827+243	Q,C4	0.939	PBE06	0.24 ± 0.15	PBE06	11.2 ± 6.98	–	–
0827+243	Q,C5	0.939	PBE06	0.24 ± 0.16	PBE06	11.2 ± 7.45	–	–
0827+243	Q,C6	0.939	PBE06	0.06 ± 0.07	PBE06	2.8 ± 3.26	–	–
0828+493	B	0.548	GPC99	0.34	GPC99	10.3	0.665	Fos98
0829+046	B,C1	0.18	JM01	1.4 ± 0.2	JM01	15.3 ± 2.18	–	–
0829+046	B,C2	0.18	JM01	0.82 ± 0.21	JM01	8.95 ± 2.29	–	–
0829+046	B,C3	0.18	JM01	0.7 ± 0.1	JM01	7.64 ± 1.09	–	–
0829+046	B,C4	0.18	JM01	0.37 ± 0.02	JM01	4.04 ± 0.22	–	–
0833+654	Q _l	1.112	VC94	-0.02	VC94	-1.05	0.023	VC94
0835+580	Q _l	1.534	VC94	-0.01	VC94	-0.65	0.023	VC94
0836+710	Q _{l,B}	2.172	VC94	0.23 ± 0.05	VC94	18.4 ± 4	2.4	HF04
0836+710	Q _{c,D}	2.172	VC94	0.14 ± 0.05	VC94	11.2 ± 4	–	–
0839+616	Q _l	0.862	VC94	0 ± 0.03	VC94	0 ± 1.31	0.034	VC94
0850+581	Q _l	1.322	VC94	0.12 ± 0.02	VC94	7.13 ± 1.19	1.2	HF04
0851+202	B,K1	0.306	VC94	0.2 ± 0.03	VC94	3.59 ± 0.54	–	–
0851+202	B,K2	0.306	VC94	0.27 ± 0.03	VC94	4.85 ± 0.54	1.2	HF04
0906+430	Q _{c1,A}	0.67	VC94	0.013	VC94	0.46	–	–
0906+430	Q _{c1,B}	0.67	VC94	0.18 ± 0.03	VC94	6.43 ± 1.07	0.92	Fos98
0917+449	B,B	2.18	JM01	0.15 ± 0.02	JM01	12.04 ± 1.6	1.2	HF04
0923+392	Q,B	0.698	VC94	0.18 ± 0.01	VC94	6.65 ± 0.37	11.2	HF04
0923+392	Q,D	0.698	VC94	0.022	VC94	0.81	–	–
0953+254	Q,C	0.712	Kell04	0.1	Kell04	3.75	1.3	HF04
1012+232	Q,B	0.565	Kell04	0.27 ± 0.02	Kell04	8.37 ± 0.62	1.1	HF0
1015+359	Q,B	1.226	Kell04	0.21 ± 0.04	Kell04	11.9 ± 2.26	–	–
1038+528	Q,C1	0.678	OWW80	0.14	Marc88	5.05	0.7	Gur99
1038+528	Q,C2	2.296	OWW80	0.18	Marc88	14.8	–	–
1039+811	Q _c	1.26	VC94	0.07	VC94	4.03	1.1	HF04
1040+123	Q _{c1}	1.028	VC94	0.11 ± 0.05	VC94	5.48 ± 2.49	0.86	VC94
1055+018	Q,C2	0.888	IT90	0.19 ± 0.05	Kell98	8.49 ± 2.23	4.1	HF04
1101+384	B	0.031	VC94	1.33 ± 0.02	VC94	2.59 ± 0.04	–	–
1127-145	Q _{p,C1}	1.187	JM01	0.52 ± 0.16	JM01	28.7 ± 8.83	0.78	Fos98
1127-145	Q _{p,C2}	1.187	JM01	0.27 ± 0.05	JM01	14.9 ± 2.76	–	–
1137+660	Q _l	0.646	VC94	0.06 ± 0.02	VC94	2.08 ± 0.69	0.13	VC94
1144+35	B,C1	0.063	Gio99a	0.49 ± 0.018	Gio99a	1.93 ± 0.07	0.67	Gur99
1144+35	B,C2	0.063	Gio99a	0.46 ± 0.018	Gio99a	1.81 ± 0.07	–	–
1150+812	Q _c	1.25	VC94	0.11 ± 0.05	VC94	6.29 ± 2.86	1.4	HF04
1156+295	Q,C1	0.73	HB89	0.39 ± 0.1	PK97	14.9 ± 3.83	1.8	HF04
1156+295	Q,C2	0.73	HB89	0.23 ± 0.05	PK97	8.81 ± 1.92	–	–
1156+295	Q,C3	0.73	HB89	0.24 ± 0.04	PK97	9.19 ± 1.53	–	–
1156+295	Q,C4	0.73	HB89	0.15 ± 0.05	PK97	5.75 ± 1.92	–	–
1219+285	B,C9	0.102	JM01	0.13	JM01	0.82	–	–
1219+285	B,C3+C8	0.102	JM01	0.32 ± 0.05	JM01	2.02 ± 0.32	0.91	Fos98
1219+285	B,C7	0.102	JM01	0.6	JM01	3.78	–	–
1219+285	B,C2+C6	0.102	JM01	0.47 ± 0.01	JM01	2.96 ± 0.06	–	–
1219+285	B,C1+C5	0.102	JM01	0.5 ± 0.07	JM01	3.15 ± 0.44	–	–
1222+216	Q _l	0.435	VC94	0.09 ± 0.04	VC94	2.22 ± 0.99	1.4	HF04
1226+023	Q _{c,C2}	0.158	VC94	1.15 ± 0.15	VC94	11.1 ± 1.45	–	–
1226+023	Q _{c,C3}	0.158	VC94	0.79 ± 0.03	VC94	7.61 ± 0.29	43.6	HF04
1226+023	Q _{c,C4}	0.158	VC94	0.99 ± 0.24	VC94	9.54 ± 2.31	–	–
1226+023	Q _{c,C5}	0.158	VC94	1.2 ± 0.03	VC94	11.56 ± 0.29	–	–
1226+023	Q _{c,C6}	0.158	VC94	0.65 ± 0.09	VC94	6.26 ± 0.87	–	–
1226+023	Q _{c,C7}	0.158	VC94	0.76 ± 0.05	VC94	7.32 ± 0.48	–	–
1226+023	Q _{c,C8}	0.158	VC94	0.92 ± 0.11	VC94	8.86 ± 1.06	–	–
1226+023	Q _{c,C8}	0.158	VC94	0.82 ± 0.12	VC94	7.9 ± 1.16	–	–
1228+127	G	0.003	VC94	1.1 ± 0.3	VC94	0.22 ± 0.06	0.86	VC94
1253-055	Q _c	0.538	VC94	0.5 ± 0.1	VC94	14.9 ± 2.97	13	HF04

Table 1 – Continued

IAU name	classification	z	references	μ	references	β_{app}	$S_{5\text{ GHz}}^{\text{ob}}(\text{Jy})$	ref
1253–055	Q _c ,C3	0.538	VC94	0.12 ± 0.02	VC94	3.57 ± 0.59	–	–
1308+326	B,K1	0.996	VC94	0.13	VC94	6.63	–	–
1308+326	B,K2	0.996	VC94	0.75	VC94	36.5	3.6	HF04
1308+326	B,K3	0.996	VC94	0.29	VC94	14.1	–	–
1322–427	G	0.0008	VC94	4.0.8	VC94	0.2 ± 0.04	0.86	VC94
1334–127	Q	0.539	IT88	0.21	ZJH00	6.25	4.4	HF04
1345+125	G,C	0.121	Kell04	0.16 ± 0.01	Kell04	1.19 ± 0.07	3.1	HF04
1345+125	G,E	0.121	Kell04	0.04 ± 0.01	Kell04	0.298 ± 0.07	–	–
1406–076	Q,C1	1.49	PBE06	0.22 ± 0.19	PBE06	14.1 ± 12.2	–	–
1406–076	Q,C2	1.49	PBE06	0.4 ± 0.09	PBE06	25.7 ± 5.78	15.1	HF04
1406–076	Q,C3	1.49	PBE06	0.32 ± 0.13	PBE06	20.5 ± 8.35	–	–
1406–076	Q,C4	1.49	PBE06	0.23 ± 0.03	PBE06	14.77 ± 1.93	–	–
1418+546	B	0.152	RJ83	0.66	GPC99	6.13	1.7	HF04
1458+718	Q _c	0.905	VC94	0.25 ± 0.15	VC94	11.33 ± 6.8	2.68	VC94
1458+718	Q _c ,B	0.905	VC94	0 ± 0.03	VC94	0 ± 1.36	–	–
1502+106	Q,J2	1.833	Fom00	0.64 ± 0.16	Fom00	46.6 ± 11.6	1.8	HF04
1502+106	Q,J3	1.833	Fom00	0.38 ± 0.26	Fom00	27.68 ± 18.9	–	–
1502+106	Q,J4	1.833	Fom00	0.18 ± 0.04	Fom00	13.1 ± 2.91	–	–
1502+106	Q,J5	1.833	Fom00	0.48 ± 0.12	Fom00	34.97 ± 8.74	–	–
1504–166	Q	0.876	IT88	0.055	ZJH00	2.43	2.8	HF04
1510–089	Q,C1	0.361	JM01	0.51 ± 0.04	JM01	10.66 ± 0.84	–	–
1510–089	Q,D1	0.361	JM01	0.28 ± 0.14	JM01	5.85 ± 2.93	–	–
1510–089	Q,D2	0.361	JM01	0.63 ± 0.1	JM01	13.17 ± 2.09	3.3	HF04
1532+016	Q,B	1.42	Kell04	0.21 ± 0.01	Kell04	13.07 ± 0.62	1.3	HF04
1548+056	Q,B	1.422	Kell04	0.12 ± 0.01	Kell04	7.48 ± 0.62	3.3	HF04
1606+106	Q	1.23	SK94	0.093	PK98	5.26	1.7	HF04
1607+268	Q _p	0.473	VC94	0 ± 0.025	VC94	0 ± 0.66	1.51	VC94
1611+343	B,C5	1.401	Von95	0.2 ± 0.02	AH01	12.34 ± 1.23	4	HF04
1611+343	B,C3	1.401	Von95	0.07 ± 0.009	AH01	4.32 ± 0.56	–	–
1611+343	B,C2	1.401	Von95	0.134 ± 0.015	AH01	8.27 ± 0.93	–	–
1618+177	Q ₁	0.555	VC94	0.1 ± 0.03	VC94	3.05 ± 0.92	0.14	VC94
1622–253	Q	0.786	JM01	0.51 ± 0.13	JM01	20.7 ± 5.28	3.5	HF04
1622–297	Q,B2+D2	0.815	JM01	0.14 ± 0.03	JM01	5.85 ± 1.25	–	–
1622–297	Q,B1+D1	0.815	JM01	0.34 ± 0.04	JM01	14.21 ± 1.67	–	–
1622–297	Q,E1	0.815	JM01	0.33 ± 0.06	JM01	13.8 ± 2.1	–	–
1622–297	Q,F2	0.815	JM01	0.3 ± 0.03	JM01	12.5 ± 1.25	–	–
1622–297	Q,F1	0.815	JM01	0.4 ± 0.29	JM01	16.7 ± 12.1	2.4	HF04
1633+382	Q,B3	1.814	JM01	0.14 ± 0.03	JM01	10.1 ± 2.17	–	–
1633+382	Q,B1	1.814	JM01	0.2 ± 0.02	JM01	14.5 ± 1.45	3.2	HF04
1637+826	G	0.023	VC94	0.05 ± 0.07	VC94	0.07 ± 0.1	0.8	VC94
1641+399	Q _c ,C2	0.594	VC94	0.47 ± 0.02	VC94	15.2 ± 0.65	8.4	HF04
1641+399	Q _c ,C3	0.594	VC94	0.3 ± 0.01	VC94	9.7 ± 0.32	–	–
1641+399	Q _c ,C4	0.594	VC94	0.31 ± 0.01	VC94	10.02 ± 0.32	–	–
1641+399	Q _c ,C5	0.594	VC94	0.23 ± 0.03	VC94	7.44 ± 0.97	–	–
1642+690	Q _c	0.751	Kell04	0.34 ± 0.04	VC94	13.3 ± 1.57	1.5	HF04
1652+398	B	0.034	JM01	0.96 ± 0.1	JM01	2.05 ± 0.21	1.4	HF04
1655+077	Q,B	0.621	Kell04	0.43 ± 0.03	Kell04	14.4 ± 1.01	1.6	HF04
1655+077	Q,C	0.621	Kell04	0.14 ± 0.02	Kell04	4.7 ± 0.67	–	–
1721+343	Q ₁ ,B	0.206	VC94	0.16 ± 0.05	VC94	1.99 ± 0.62	–	–
1721+343	Q ₁ ,C	0.206	VC94	0.28 ± 0.03	VC94	3.48 ± 0.37	0.47	VC94
1730–130	Q,B2	0.9	JM01	0.23 ± 0.02	JM01	10.4 ± 0.9	–	–
1730–130	Q,B1	0.9	JM01	0.28 ± 0.1	JM01	12.6 ± 4.51	7	HF04
1749+096	B	0.322	RJ83	1	Igu00	18.8	2.3	HF04
1749+701	B	0.77	VC94	0.26 ± 0.03	VC94	10.4 ± 1.2	1.02	Fos98
1800+440	Q,B	0.663	Kell04	0.49 ± 0.04	Kell04	17.4 ± 1.42	1.1	HF04
1803+784	B	0.684	VC94	0.004 ± 0.03	VC94	0.15 ± 1.02	2.6	HF04
1823+568	B	0.664	VC94	0.12	VC94	4.26	1.5	HF04
1828+487	Q _c ,A	0.691	VC94	0.38 ± 0.025	VC94	13.9 ± 0.92	6.59	VC94
1828+487	Q _c ,B	0.691	VC94	0.23 ± 0.04	VC94	8.43 ± 1.47	–	–
1830+285	Q ₁ ,B	0.594	VC94	0.13 ± 0.04	VC94	4.2 ± 1.29	1.5	HF04

Table 1 – Continued

IAU name	classification	z	references	μ	references	β_{app}	$S_{5 \text{ GHz}}^{\text{ob}} (\text{Jy})$	ref
1830+285	Q _l ,C	0.594	VC94	0.13 ± 0.04	VC94	4.2 ± 1.29	–	–
1845+797	G,B	0.057	Kell04	0.55 ± 0.03	Kell04	1.96 ± 0.11	–	–
1845+797	G,C	0.057	Kell04	0.61 ± 0.02	Kell04	2.17 ± 0.07	4.41	Gur99
1901+319	Q _c ,C2	0.635	VC94	0 ± 0.03	VC94	0 ± 1.03	–	–
1901+319	Q _c ,C3	0.635	VC94	0.64 ± 0.1	VC94	21.9 ± 3.42	1.9	HF04
1908–201	B,C2	0.2	JM01	1.2 ± 0.1	JM01	14.5 ± 1.21	2.3	HF04
1928+738	Q _c ,A1	0.302	VC94	0.32 ± 0.1	VC94	5.68 ± 1.78	–	–
1928+738	Q _c ,B	0.302	VC94	0.37 ± 0.05	VC94	6.57 ± 0.89	–	–
1928+738	Q _c ,C	0.302	VC94	0.34 ± 0.03	VC94	6.04 ± 0.53	–	–
1928+738	Q _c ,C2	0.302	VC94	0.51 ± 0.1	VC94	9.06 ± 1.78	–	–
1928+738	Q _c ,C3	0.302	VC94	0.57 ± 0.05	VC94	10.1 ± 0.89	3.6	HF04
1928+738	Q _c ,C4	0.302	VC94	0.4 ± 0.05	VC94	7.1 ± 0.89	–	–
1928+738	Q _c ,C6	0.302	VC94	0.4 ± 0.1	VC94	7.1 ± 1.78	–	–
1928+738	Q _c ,C7	0.302	VC94	0.6 ± 0.1	VC94	10.66 ± 1.78	–	–
1928+738	Q _c ,C9	0.302	VC94	0.31 ± 0.55	VC94	5.51 ± 9.77	–	–
1934–638	Q _p	0.183	VC94	0.01 ± 0.03	VC94	0.11 ± 0.33	6	VC94
1951+498	Q _l	0.466	VC94	0.07	VC94	1.84	0.09	VC94
1957+405	G,D	0.056	Kell04	0.18 ± 0.02	Kell04	0.63 ± 0.07	–	–
1957+405	G,E	0.056	Kell04	0.19 ± 0.03	Kell04	0.66 ± 0.11	–	–
1957+405	G,F	0.056	Kell04	0.22 ± 0.03	Kell04	0.77 ± 0.11	0.74	Gur99
1957+405	G,G	0.056	Kell04	0.16 ± 0.03	Kell04	0.56 ± 0.11	–	–
2005+403	Q,B	1.736	Kell04	0.2 ± 0.03	Kell04	14.1 ± 2.12	7.4	Dav94
2007+777	B	0.342	VC94	0.18 ± 0.04	VC94	3.58 ± 0.79	1.7	HF04
2021+614	Q _p	0.227	VC94	0.022 ± 0.022	VC94	0.3 ± 0.3	3	HF04
2113+293	Q,B	1.514	Kell04	0.04 ± 0.01	Kell04	2.59 ± 0.65	1.2	HF04
2145+067	Q,C	0.999	Kell04	0.03 ± 0.01	Kell04	1.46 ± 0.49	6.4	HF04
2200+420	B,S1	0.069	VC94	1.2 ± 0.1	VC94	5.16 ± 0.43	5.6	HF04
2200+420	B,S2	0.069	VC94	1.1 ± 0.1	VC94	4.73 ± 0.43	–	–
2200+420	B,S3	0.069	VC94	1.1 ± 0.1	VC94	4.73 ± 0.43	–	–
2200+420	B,S5	0.069	VC94	1 ± 0.1	VC94	4.3 ± 0.43	–	–
2201+315	Q,B	0.298	Kell04	0.34 ± 0.03	Kell04	5.96 ± 0.53	2.9	HF04
2223–052	Q,B	1.404	Kell04	0.5 ± 0.08	Kell04	30.9 ± 4.94	–	–
2223–052	Q,C	1.404	Kell04	0.31 ± 0.03	Kell04	19.2 ± 1.85	6.4	HF04
2230+114	Q _p	1.037	JM01	0.33 ± 0.01	JM01	16.5 ± 0.5	–	–
2230+114	Q _p	1.037	JM01	0.34 ± 0.04	JM01	17.05 ± 2.01	1.46	Fos98
2230+114	Q _p	1.037	JM01	0.25 ± 0.01	JM01	12.5 ± 0.5	–	–
2243–123	Q _c	0.63	BSB75	0.19	ZJH00	6.45	2.7	HF04
2251+158	Q _p ,C2	0.859	VC94	0.045 ± 0.016	VC94	1.97 ± 0.7	–	–
2251+158	Q _p ,C3	0.859	VC94	-0.046 ± 0.072	VC94	-2 ± 3.14	–	–
2251+158	Q _p ,C4	0.859	VC94	0.35 ± 0.06	VC94	15.2 ± 2.61	16	HF04
2251+158	Q _p ,C5	0.859	VC94	0.21 ± 0.05	VC94	9.14 ± 2.18	–	–
2345–167	Q	0.576	ZJH00	0.08 ± 0.03	Hong99	2.52 ± 0.95	2.03	Fos98
2352+495	Q _c ,A	0.237	VC94	0.03	VC94	0.425	1.6	Gur99
2352+495	Q _c ,B2	0.237	VC94	0.03	VC94	0.425	–	–

References: 1: Bec91; Becker et al. (1991); BK05: Bach et al. (2005); BSB75: Browne et al. (1975); BW99: Britzen et al. (1999); Dav94: Davis (1994); Fom00: Fomalont et al. (2000); Fos98: Fossati et al. (1998); Gio99a: Giovannini et al. (1999); GPC99: Gabuzda et al. (1999); Gur99: Gurvits et al. (1999); HB89: Hewitt & Burbidge (1989); HF04: Horiuchi et al. (2004); Hong99: Hong et al. (1999); Igu00: Iguchi et al. (2000); IT88: Impey & Tapia (1988); IT90: Impey & Tapia (1990); JM01: Jorstad et al. (2001); Kell98: Kellermann et al. (1998); Kell04: Kellermann et al. (2004); Mil78a: Miller (1978); OWW80: Owen et al. (1980); PBE06: Piner et al. (2006); PJW76: Peterson et al. (1976); PK97: Piner & Kingham (1997); PK06: Pyatunina et al. (2006); PMM00: Pyatunina et al. (2000); Pya98: Pyatunina (1998); Pya03: Pyatunina et al. (2003); RJ83: Rudnick & Jones (1983); SWH97: Shen et al. (1997); SHW98: Shen et al. (1998); SK94: Stickel & Kuhr (1994); SRK96: Stickel et al. (1996); VC94: Vermeulen & Cohen (1994); Von95: Von et al. (1995); Zen02: Zensus et al. (2002); ZJH00: Zhou et al. (2000).

2.2.2 The Characteristic of β_{app}

From the proper motion and Equation (1), we have calculated β_{app} in the Λ -CDM model. Figure 2 shows the number distribution of β_{app} for the three types of objects. We see that the β_{app} distribution for the whole

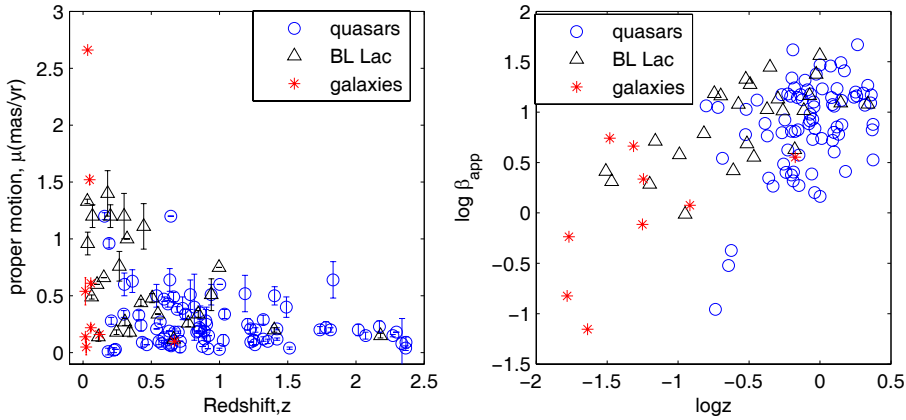


Fig. 1 Left panel shows the relation between the proper motion and the redshift. Right panel, that between β_{app} and the redshift (a log-log plot). The three types of objects are marked differently.

sample is mainly between 0 to 20, with a tail extending up to ~ 45 . A linear regression of β_{app} on z (in logarithms) gives,

$$\log \beta_{app} = (0.59 \pm 0.13) \log z + (0.94 \pm 0.18), \quad (2)$$

and a linear correlation coefficient of 0.60, a chance probability of $p = 3.2 \times 10^{-5}$ (see Fig. 1). When we consider the three types separately, we obtain linear correlation coefficients of 0.43 for the quasars, 0.66 for the BL Lacs and 0.21 for the galaxies.

2.2.3 The Relation between 5 GHz Flux Density and Redshift

The emissions in AGNs are obviously beamed, and we can use the sample to examine the beaming effect by considering the relationship between the flux density and the redshift. From the observed data ($S_{5\text{GHz}}^{\text{ob}}$) listed in the table above, we K-corrected the flux density using $S = S^{\text{ob}}(1+z)^{\alpha-1}$ ($\alpha = 0.0$ is adopted for the radio band). Then we have

$$\log \frac{S_{5\text{GHz}}^{\text{ob}}}{1+z} = -0.25 \log z + 0.21, \quad (3)$$

with a linear correlation coefficient of -0.28. As Figure 3 shows, there is no correlation. The reason may be due to the fact that the emission is amplified by the relativistic effect (Kembhavi & Narlikar 1999). Assume a relativistic luminous plasma blob with velocity $\beta_{\text{in}} = v/c$ and Lorentz factor $\gamma = (1 - \beta_{\text{in}}^2)^{-1/2}$ (Cohen, Lister & Vermeulen 2005), at an angle θ to the line-of-sight (LOS), then its Doppler factor δ is

$$\delta = \frac{1}{\gamma(1 - \beta_{\text{in}} \cdot \cos \theta)}. \quad (4)$$

Based on the beaming model, we have (Fan et al. 1996)

$$S_{5\text{GHz}}^{\text{ob}} = \delta^{3+\alpha} S_{5\text{GHz}}^{\text{in}}, \quad (5)$$

$$\beta_{app} = \beta_{\text{in}} \cdot \sin \theta / (1 - \beta_{\text{in}} \cdot \cos \theta) = \delta \cdot \sin \theta \cdot \beta_{\text{in}} / (1 - \beta_{\text{in}}^2)^{0.5}, \quad (6)$$

where $S_{5\text{GHz}}^{\text{ob}}$ and $S_{5\text{GHz}}^{\text{in}}$ are respectively the observed and intrinsic (corrected) flux densities, α is the spectral index (Fan et al. 1996). For a single group of objects, we have

$$\log S_{5\text{GHz}}^{\text{in}} = -2 \log z + c, \quad (7)$$

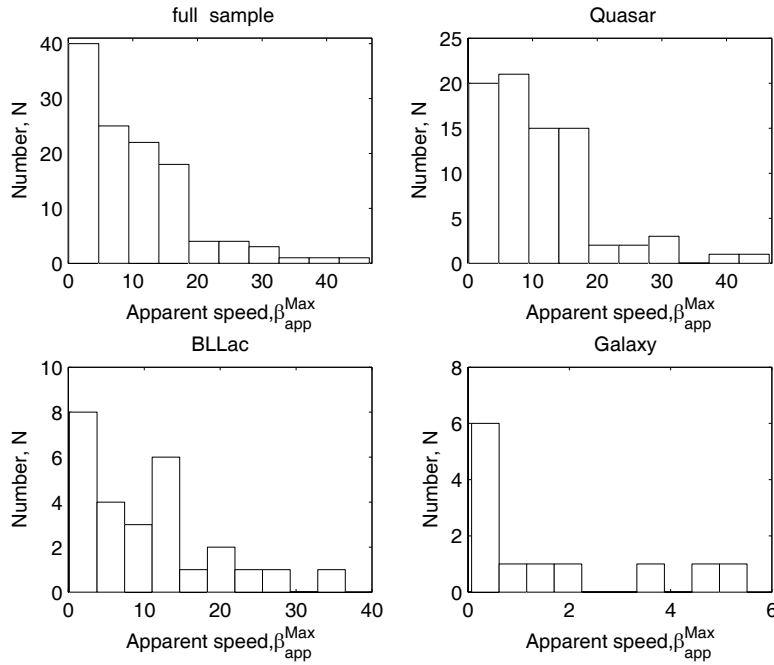


Fig. 2 Number distribution of β_{app} in the three types of objects.

and

$$\log \frac{S_{5 \text{ GHz}}^{\text{ob}}}{1+z} + 2 \log z = (3 + \alpha) \log \delta. \quad (8)$$

In the case of very small angle θ , i.e. $\sin \theta \sim (1 - \beta_{\text{in}}^{-0.5})$, we have $\delta \sim \beta_{\text{app}}$ for the expected radio flux (here $\alpha = 0$ is adopted)

$$\log \frac{S_{5 \text{ GHz}}^{\text{ob}}}{1+z} - 3 \log \beta_{\text{app}} = -2 \log z + c. \quad (9)$$

From the relevant data in the present paper, we obtain

$$\log \frac{S_{5 \text{ GHz}}^{\text{ob}}}{1+z} - 3 \log \beta_{\text{app}} = -(2.03 \pm 0.11) \log z - (4.34 \pm 0.31), \quad (10)$$

with a linear correlation coefficient of -0.59 and a chance probability of $p = 6.1 \times 10^{-5}$. When we consider the three types separately, we have that the linear correlation coefficient is -0.44 for the quasars, -0.68 for the BL Lacs and -0.19 for the galaxies, respectively.

3 DISCUSSION AND CONCLUSIONS

In a Friedmann cosmology (Cohen et al. 1988; Vermeulen & Cohen 1994), the proper motion decreases with increasing redshift in superluminal sources (Vermeulen & Cohen 1994; Cohen et al. 2005). For the present sample, we have (from Fig. 1) $\log \mu = -(0.28 \pm 0.11) \log z - (0.75 \pm 0.28)$, which shows that our result is consistent with that of Cohen et al. (2005). From our separate analyses of the three types of objects we found that the proper motions increase in the order, quasars — BL Lacs — galaxies. The distribution of β_{app} found by Kellermann et al. (2003) is mainly between 0 and 10, plus a tail extending to $\beta_{\text{app}} \sim 34$. Thus, our results are consistent with theirs.

For the relation between the flux density and the redshift, Fan et al. (1996) used a sample of 48 superluminal sources and found $S_{5 \text{ GHz}}^{\text{ob}} = -(0.13 \pm 0.03) \log z + c$. From the present sample we found

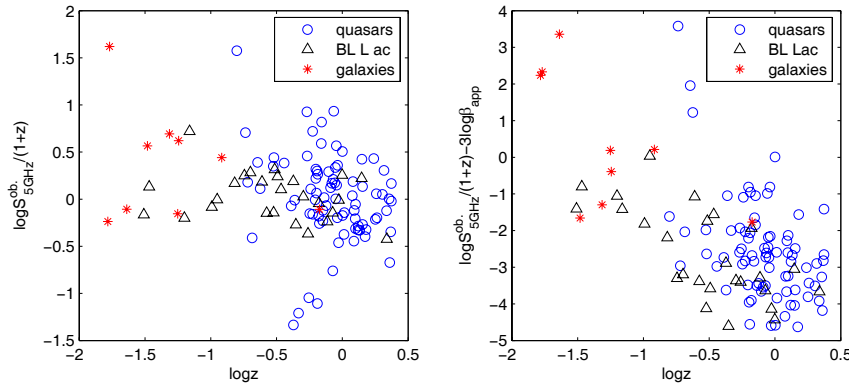


Fig. 3 Relations between $\log S_{5\text{GHz}}^{\text{ob}}/(1+z)$ and $\log z$, $\log S_{5\text{GHz}}^{\text{ob}}/(1+z) - 3 \log \beta_{\text{app}}$ and $\log z$.

$\log S_{5\text{GHz}}^{\text{ob}}/(1+z) = -0.25 \log z + 0.21$ (see Fig. 3). When the beaming effect is considered, we found that the corrected flux density is closely correlated with the redshift: $\log S_{5\text{GHz}}^{\text{ob}}/(1+z) - 3 \log \beta_{\text{app}} = -2.03 \log z - 4.34$, which is entirely consistent with the expected result, $\log S^{\text{in}} - 3 \log \beta_{\text{app}} = -2 \log z + c$. In addition, our result was obtained in the case where $\delta \sim \beta_{\text{app}}$, i.e., where the superluminal motion and the relativistic beaming boosting are nearly the same.

In this paper, 1) we collected a sample of 123 superluminal sources (84 quasars, 27 BL Lac objects and 12 galaxy objects); 2) we calculated their apparent velocities, compared some parameters amongst quasars, BL Lac objects and galaxies, and found that for the three subclasses the proper motion increases in the order, quasars — BL Lacs — galaxies; and 3) we investigated the relation between the radio flux density and redshift and found that the correlation with the redshift is much tighter for the intrinsic (corrected) flux density than for the observed flux density, and that the relativistic beaming boosting effect is, to some extend, the same with the superluminal motion.

Acknowledgements This work is partially supported by the NSFC (Grants 10573005 and 10633010), and the 973 project (2007CB815405).

References

- An T., Hong X. Y., Wang W. H., Jiang D. R., Chen Y. J., 2001, Chin. J. Astron. Astrophys. (ChJAA), 1, 305
- Bach U., Krichbaum T. P., Ros E. et al., 2005, A&A, 433, 815
- Becker R. H., White R. L., Edwards A. L., 1991, ApJS, 75, 1
- Blandford R. D., McKee C. F., Rees M. J., 1977, Nature, 267, 211
- Browne I. W. A., Savage A., Bolton J. G., 1975, MNRAS, 173, 87
- Britzen S., Witzel A., Krichbaum T. P. et al., 1999, A&A, 341, 418
- Cohen M. H., Linfield R. P., Moffet A. T. et al., 1977, nature, 268, 405
- Cohen M. H., Barthel P. D., Pearson T. J. et al., 1988, ApJ, 329, 1
- Cohen M. H., Lister M. L., Vermeulen R. C., 2005, EAS, 15, 93
- Davis R. J., 1994, Ap& SS, 216, 67
- Fan J. H., Xie G. Z., Wen S. L., 1996, A&AS, 116, 409
- Fan J. H., Xie G. Z., Bacon R., 1999, A&AS, 136, 13
- Fan J. H., Wang Y. J., Yang J. H., Su C. Y., 2004, Chin. J. Astron. Astrophys. (ChJAA), 4, 533
- Fan J. H., Romero G. E., Wang, Y. X. et al., 2005, Chin. J. Astron. Astrophys. (ChJAA), 5, 457
- Fomalont E. B., Frey S., Paragi Z. et al., 2000, ApJS, 131, 95
- Fossati G., Maraschi L., Celotti A. et al., 1998, MNRAS, 299, 433
- Gabuzda D. C., Pushkarev A. B., Cawthorne T. V., 1999, MNRAS, 307, 725
- Giovannini G., Taylor G. B., Arbizzani E. et al., 1999a, ApJ, 522, 101

- Gurvits L. I., Kellermann K. I., Frey S., 1999, A&A, 342, 378
 Hartman R. C., Bertsch D. L., Bloom S. D. et al., 1999, ApJS, 123, 79
 Hewitt A., Burbidge G., 1989, ApJS, 69, 1
 Hong X. Y., Venturi T., Wan T. S. et al., 1999, A&AS, 134, 201
 Horiuchi S., Fomalont E. B., Taylor W. K. et al., 2004, ApJ, 616, 110
 Iguchi S., Fujisawa K., Kameno S. et al., 2000, PASJ, 52, 1037
 Impey C. D., Tapia S., 1988, AJ, 333, 666
 Impey C. D., Tapia S., 1990, ApJ, 354, 124
 Jorstad, S. G., Marscher A. P., Mattox J. R. et al., 2001, ApJS, 134, 181
 Kellermann K. I., Vermeulen R. C., Zensus J. A. et al., 1998, AJ, 115, 1295
 Kellermann K. I., Lister M. L., Homan D. C. et al., 2003, ASPC, 299, 117
 Kellermann K. I., Lister M. L., Homan D. C. et al., 2004, ApJ, 609, 539
 Kembhavi A. K., Narlikar J. V., 1999, Quasars and active galactic nuclei, Cambridge University Press., ISBN 0521474779
 Marcaide J. M., Shapiro I. I., Corey B. E. et al., 1985, A&A, 142, 71
 Miller H. R., 1978a, ApJ, 223, 67
 Owen F. N., Wills B. J., Wills D., 1980, ApJ, 235, 57
 Pearson T. J., Zensus J. A., 1987, JBA&A, 98, 48
 Pedro R. C., Priyamvada N., 2007, NJPh, 9, 445
 Peterson B. A., Jauncey D. J., Wright A. E. et al., 1976, ApJ, 207, 5
 Piner B. G., Kingham K. A., 1997, ApJ, 485, L61
 Piner B. G., Kingham K. A., 1998, ApJ, 507, 706
 Piner B. G., Bhattacharai D., Edwards P. G. et al., 2006, ApJ, 640, 196
 Pyatunina T. B., 1998, ASPC, 144, 157
 Pyatunina T. B., Marchenko S. G., Marscher A. P. et al., 2000, A&A, 358, 451
 Pyatunina T. B., Rachimov I. A., Zborovskii A. A. et al., 2003, High Energy Blazar Astronomy, ASPC, 299, 89
 Pyatunina T. B., Kudryavtseva N. A., Gabuzda D. C. et al., 2006, MNRAS, 373, 1470
 Rudnick L., Jones T. W., 1983, AJ, 88, 518
 Shen Z. Q., Wan T. S., Hong X. Y., 1997, Chin. J. Astron. Astrophys. (ChJAA), 21, 158
 Shen Z. Q., Hong X. Y., Wan T. S., 1998, Chin. J. Astron. Astrophys. (ChJAA), 22, 133
 Shen Z. Q., Jiang D. R., Kameno S. et al., 2001, A&A, 370, 65
 Shen Z. Q., Shang L. L., Cai H. B. et al., 2005, ApJ, 622, 811
 Stickel M., Rieke G. H., Kuhr H. et al., 1996, ApJ, 468, 556
 Stickel M., Kuhr H., 1994, A&AS, 105, 67
 Vermeulen R. C., Cohen M. H., 1994, ApJ, 430, 467
 Von M. C., Bertsch D. L., Chiang J. et al., 1995, ApJ, 440, 525
 Xie G. Z., Dai B. Z., Mei D. C. et al., 2001, Chin. J. Astron. Astrophys. (ChJAA), 1, 213
 Zensus J. A., Ros E., Kellermann K. I. et al., 2002, AJ, 124, 662
 Zhou J. F., Jiang D. R., Hong X. Y. et al., 2000, In: EVN Symposium 2000, Proceedings of the 5th european VLBI Network Symposium held at Chalmers University of Technology, Gothenburg, Sweden, June 29 - July 1, 2000, eds. J. E. Conway et al., published Onsala Space Observatory, p.31